

Effect of Temperature on the Morphology and Kinetics of Surface Pattern Formation in Thin Block Copolymer Films

Archie P. Smith,[†] Jack F. Douglas,* Eric J. Amis, and Alamgir Karim*

Polymers Division, National Institute of Standards and Technology, Gaithersburg, Maryland 20899

Received April 13, 2007. In Final Form: July 27, 2007

Hole formation and growth on the *top layer* of thin symmetric diblock copolymer films, forming an ordered lamellar structure parallel to the solid substrate (silicon wafer) within these films, is investigated as a function of time (t), temperature (T), and film thickness (l), using a high-throughput experimental technique. The kinetics of this surface pattern formation process is interpreted in terms of a first-order reaction model with a time-dependent rate constant determined uniquely by the short-time diffusive growth kinetics characteristic of this type of ordering process. On the basis of this model, we conclude that the average hole size, λ_h , approaches a *steady-state* value, $\lambda_h(t \rightarrow \infty) \equiv \lambda_{h,\infty}(T)$, after long annealing times. The observed change in $\lambda_{h,\infty}(T)$ with temperature is consistent with a reduction of the surface elasticity (Helfrich elastic constant) of the outer block copolymer layer with increasing temperature. We also find that the time constant, $\tau(T)$, characterizing the rate at which $\lambda_h(t)$ approaches $\lambda_{h,\infty}(T)$, first decreases and then increases with increasing temperature. This temperature variation of $\tau(T)$ is attributed to two basic competing effects that influence the rate of ordering in block copolymer materials: the reduction in molecular mobility at low temperatures associated with glass formation and a slowing of the rate of ordering due to fluctuation effects associated with an approach to the block copolymer film disordering temperature (T_d) from below.

Introduction

Pattern formation in lamellae-forming films is a ubiquitous phenomenon with important ramifications in technological applications as well as for understanding the function and properties of biological membranes. The in-plane pattern formation in such films often includes a progression between island, labyrinthine, and hole patterns in addition to smooth films depending on the surface coverage.^{1,2} Such structures are seen in self-assembled monolayers,^{3–6} Langmuir films,⁷ end-tethered polymer layers,⁸ and block copolymer films.^{1,2,9–21} The existence of these patterns can be expected to have a large impact on the

properties of these films—roughness, wettability, optical transparency, rigidity, permeability, etc. It is therefore important to understand what factors influence the formation of these surface patterns so that the thin film properties can be determined and controlled.

Block copolymer (BC) film surfaces provide a particularly important example of this type of surface pattern formation. The relatively large scale of the surface patterns (normally much larger than the macromolecular dimensions) and their corresponding slow growth facilitate the determination of the pattern geometry and coarsening kinetics. Moreover, it is also possible to vary the relative molecular masses of the block components, the total molecular mass, polymer components, and other molecular variables to investigate models of this pattern formation and facilitate the development of fundamental theories to describe this type of pattern formation. We anticipate that many aspects of pattern formation in block copolymer films should be broadly applicable to other lamellae-forming films.

Block copolymer film pattern formation is a complex phenomenon and the relevant parameter space is rather large. To more efficiently explore this phenomenon in this study, a combinatorial experimental approach is utilized. Combinatorial experiments vary several different parameters simultaneously to greatly improve experimental efficiency and throughput.^{1,2,22–24} This methodology is implemented here by creating samples with a continuous, controlled gradient in film thickness, l , that are annealed on a temperature (T) gradient orthogonal to the l -gradient. These gradient films can be prepared with different molecular mass (M) polymers, so that numerous measurements

* To whom correspondence should be sent. E-mail: alamgir.karim@nist.gov (A.K.); jack.douglas@nist.gov (J.F.D.).

[†] Current address: Columbian Chemical Co., 1800 West Oak Commons Ct., Marietta, GA 30062.

(1) Smith, A. P.; Douglas, J. F.; Meredith, J. C.; Amis, E. J.; Karim, A. *Phys. Rev. Lett.* **2001**, *87*(1), 015503.

(2) Smith, A. P.; Douglas, J. F.; Meredith, J. C.; Amis, E. J.; Karim, A. *J. Polym. Sci. Part B—Polym. Phys.* **2001**, *39*, 2141–2158.

(3) Woodward, J. T.; Schwartz, D. K. *J. Am. Chem. Soc.* **1996**, *118*, 7861.

(4) Woodward, J. T.; Ulman, A.; Schwartz, D. K. *Langmuir* **1996**, *12*, 3626.

(5) Woodward, J. T.; Doudevski, I.; Sikes, H. D.; Schwartz, D. K. *J. Phys. Chem. B* **1997**, *101*, 7535.

(6) Woodward, J. T.; Gwin, H.; Schwartz, D. K. *Langmuir* **2000**, *16*, 2957.

(7) Leibler, S.; Andelman, D. *J. Phys. (Paris)* **1987**, *48*, 2013.

(8) Karim, A.; Tsukruk, V. V.; Douglas, J. F.; Satija, S. K.; Fetters, L. J.; Reneker, D. H.; Foster, M. D. *J. Phys. II (Paris)* **1995**, *5*, 1441.

(9) Henkee, C. S.; Thomas, E. L.; Fetters, L. J. *J. Mater. Sci.* **1988**, *23*, 1685.

(10) Russell, T. P.; Coulon, G.; Deline, V. R.; Miller, D. C. *Macromolecules* **1989**, *22*, 4600.

(11) Auserre, D.; Chatenay, D.; Coulon, G.; Collin, B. *J. Phys. Fr.* **1990**, *51*, 2571.

(12) Coulon, G.; Auserre, D.; Russell, T. P. *J. Phys. (Paris)* **1990**, *51*, 777.

(13) Coulon, G.; Collin, B.; Auserre, D.; Chatenay, D.; Russell, T. P. *J. Phys. (Paris)* **1990**, *51*, 2801.

(14) Russell, T. P.; Menelle, A.; Anastasiadis, S. H.; Satija, S. K.; Majkrzak, C. F. *Macromolecules* **1991**, *24*, 6263.

(15) Collin, B.; Chatenay, D.; Coulon, G.; Auserre, D.; Gallot, Y. *Macromolecules* **1992**, *25*, 1621.

(16) Menelle, A.; Russell, T. P.; Anastasiadis, S. H.; Satija, S. K.; Majkrzak, C. F. *Phys. Rev. Lett.* **1992**, *68*, 67. Arceo, A.; Green, P. F. *J. Phys. Chem.* **2005**, *109*, 6958.

(17) Cai, Z.; Huang, K.; Montano, P. A.; Russell, T. P.; Bai, J. M.; Zajac, G. W. *J. Chem. Phys.* **1993**, *93*, 2376.

(18) Coulon, G.; Collin, B.; Chatenay, D.; Gallot, Y. *J. Phys. II (Paris)* **1993**, *3*, 697.

(19) Coulon, G.; Daillant, J.; Collin, B.; Benattar, J. J.; Gallot, Y. *Macromolecules* **1993**, *26*, 1582.

(20) Mayes, A. M.; Russell, T. P.; Bassereau, P.; Baker, S. M.; Smith, G. S. *Macromolecules* **1994**, *27*, 749.

(21) Grim, P. C. M.; Nyrkova, I. A.; Semenov, A. N.; Brinke, G. T.; Hadziioannou, G. *Macromolecules* **1995**, *28*, 7501.

(22) Jandeleit, B.; Schaefer, D. J.; Powers, T. S.; Turner, H. W.; Weinberg, W. H. *Angew. Chem., Int. Ed.* **1999**, *38*, 2494.

(23) Meredith, J. C.; Smith, A. P.; Karim, A.; Amis, E. J. *Macromolecules* **2000**, *33*, 9747.

(24) Meredith, J. C.; Karim, A.; Amis, E. J. *Macromolecules* **2000**, *33*, 5760.

of the effect of l and T on BC pattern formation are simultaneously acquired from a single film. By exploiting combinatorial methods in this work, the effects of l , T , and M on block copolymer pattern formation are found and incorporated into a proposed theory of pattern formation in generic lamellae-forming films.

Background

Block copolymers are systems having blocks of different polymers covalently linked together. The extent of segregation of the blocks can be expressed in terms of the parameter χN , where χ is the Flory–Huggins interaction parameter, related to the incompatibility of the monomers, and N is the degree of polymerization.^{25,26} If the value of χN is above a given value (≈ 10.5 for block copolymers) the system will microphase separate into an “ordered” state. This transition is termed an order–disorder transition, and the transition temperature where this phase transition occurs is designated the order–disorder transition (ODT) temperature (T_d). For a given polymer system, χ is dependent on temperature and will generally decrease with increasing T such that a transition between the ordered and disordered state will occur when the critical value of χN is crossed. The morphology formed upon ordering depends on the relative volumes of each block and can include spheres, cylinders, cocontinuous, and lamellar morphologies.²⁶ For blocks with nearly equal volumes or symmetric block copolymers, lamellae are usually formed having a thickness (L_0) that depends on N .

When these symmetric materials are cast as thin films, the thermodynamic interactions between the different blocks and the substrate are found to influence both the morphology and order–disorder transition temperature.^{9–21,27–38} In general, one block will have an energetic preference for the substrate and the lamellae will form parallel to the substrate surface with a thickness equal to L_0 . This formation of lamellae parallel to the substrate affects both the observed ODT and the film morphology formed. T_d is found to increase since the preference for the substrate by one of the blocks has to be overcome for the system to disorder.^{16,32,38} As the film becomes thinner, the total number of lamellae decreases and this effect becomes stronger.¹⁶ The morphology is affected since L_0 is constant and a smooth film can only form when the film thickness is an integral multiple of L_0 . This smooth film has a thickness of $l_s = mL_0$ (m an integer) when one block prefers both the substrate and air interfaces and $l_s = (m + 1/2)L_0$ when one block prefers the substrate and the other block prefers the air interface. When the film thickness deviates substantially from these characteristic values, an incomplete surface lamella forms when the system orders. This

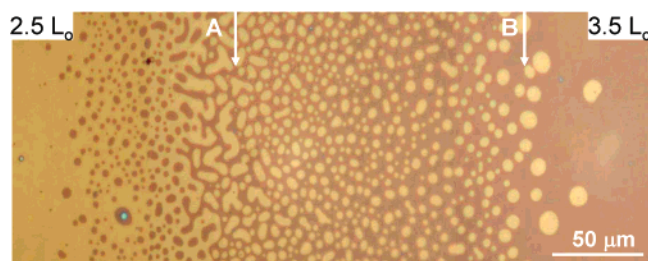


Figure 1. Optical micrograph obtained from a block copolymer thin film gradient that varies from $2.5L_0$ to $3.5L_0$ in l showing the progression from smooth to islands to labyrinthine to holes to smooth surface morphology. Arrows designate the approximate locations of the (A) 53 nm film and (B) 80 nm film along this continuous morphology variation.

incomplete lamella consists of islands or holes of height L_0 with the exact morphology governed by the difference $l - l_s$, and an example of this surface pattern formation is shown in Figure 1. This figure contains an optical micrograph of a thin film having an l -gradient varying from $2.5L_0$ to $3.5L_0$ showing the morphology progression from smooth, to islands, to labyrinthine, to holes, and finally back to smooth surfaces as l is increased.

Although this phenomenon has been observed repeatedly, no complete theory of pattern formation in BC films exists. Interesting models and ideas, however, have been proposed that can serve as the basis for developing a more refined theoretical description. The most developed model for BC film surface pattern formation proposes that the pattern formation corresponds to a type of two-dimensional “phase separation”. Here, film thickness relative to a critical value (l_s) is analogous to the compositional order parameter in the traditional fluid mixtures.^{12,21,33,39–42} Indeed, the early stage morphology and kinetics of BC pattern formation superficially resemble those observed in phase-separated polymer blend films. This model predicts patterns resembling spinodal decomposition for certain film thickness ranges, which have been observed,^{1,2,34,36,42} lending credence to this model.

Recent experimental observations of a tendency for the BC patterns to approach a constant size at long times, but the dependence of the pattern size on molecular mass² cannot be explained within the basic phase separation model. To account for these observations, surface elasticity considerations can be incorporated into the model.² Previous theoretical work has indicated that surface elasticity can limit the scale of pattern formation in surfactant films.^{7,43} In addition, preliminary evidence of a (possibly transient) pinning of the scale of phase separation has been observed in Cahn–Hilliard type simulations that incorporate surface elasticity.⁴⁴ On the basis of these findings, the inclusion of surface elasticity in a theory of pattern formation in BC films can be expected to limit the size of the surface

(25) Bates, F. S.; Frederickson, G. H. *Annu. Rev. Phys. Chem.* **1990**, *41*, 525.

(26) Hamley, I. W. *The Physics of Block Copolymers*; Oxford University Press: Oxford, 1998.

(27) Hasegawa, H.; Hashimoto, T. *Macromolecules* **1985**, *8*, 589.

(28) Green, P. F.; Christensen, T. M.; Russell, T. P.; Jerome, R. *Macromolecules* **1989**, *22*, 2189.

(29) Anastasiadis, S. H.; Russell, T. P.; Satija, S. K.; Majkrzak, C. F. *J. Chem. Phys.* **1990**, *92*, 5677.

(30) Green, P. F.; Christensen, T. M.; Russell, T. P.; Jerome, R. *J. Chem. Phys.* **1990**, *92*, 1478.

(31) Green, P. F.; Christensen, T. M.; Russell, T. P. *Macromolecules* **1991**, *24*, 252–255.

(32) Russell, T. P.; Menelle, A.; Anastasiadis, S. H.; Satija, S. K.; Majkrzak, C. F. *Macromol. Chem., Macromol. Symp.* **1992**, *62*, 157.

(33) Bassereau, P.; Brodbeck, D.; Russell, T. P.; Brown, H. R.; Shull, K. R. *Phys. Rev. Lett.* **1993**, *71*, 1716.

(34) Mansky, P.; Russell, T. P.; Hawker, C. J.; Pitsikalis, M.; Mays, J. *Macromolecules* **1997**, *30*, 6810.

(35) Mansky, P.; Russell, T. P.; Hawker, C. J.; Mays, J.; Cook, D. C.; Satija, S. K. *Phys. Rev. Lett.* **1997**, *79*, 237.

(36) Heier, J.; Sivaniah, E.; Kramer, E. J. *Macromolecules* **1999**, *32*, 9007.

(37) Heier, J.; Genzer, J.; Kramer, E. J.; Bates, F. S.; Walheim, S.; Krausch, G. *J. Chem. Phys.* **1999**, *111*, 11101.

(38) Mutter, R.; Stuhn, B. *Macromolecules* **1995**, *28*, 5022.

(39) Joly, S.; Raquois, A.; Paris, F.; Hamdoun, B.; Auvray, L.; Auserre, D.; Gallot, Y. *Phys. Rev. Lett.* **1996**, *77*, 4394.

(40) Vignaud, G.; Gibaud, A.; Grubel, G.; Joly, S.; Auserre, D.; Legrand, J. F.; Gallot, Y. *Phys. B* **1998**, *248*, 250.

(41) Mansky, P.; Tsui, O. K. C.; Russell, T. P.; Gallot, Y. *Macromolecules* **1999**, *32*, 4832.

(42) Maaloum, M.; Auserre, D.; Chatenay, D.; Gallot, Y. *Phys. Rev. Lett.* **1993**, *70*, 2577.

(43) Seul, M.; Andelman, D. *Science* **1995**, *267*, 476.

(44) Jiang, Y.; Lookman, T.; Sayers, A. B.; Douglas, J. F. Unpublished. The Cahn–Hilliard model of phase separation in combination with the Helfrich model of the surface elasticity shows that the scale of the film phase separation pattern can “pin”, at least transiently, at long times due to surface elasticity. See also references 43 and 58. There are also interesting simulations of elastic effects in alloy phase separation (Onuki, A.; Nishimori, H. *Phys. Rev. B* **1991**, *43*, 13649.), which show that elasticity can modify the coarsening dynamics from the conventional one-third power scaling of “ordinary” phase separation. Smaller apparent coarsening exponents are reported in this work.

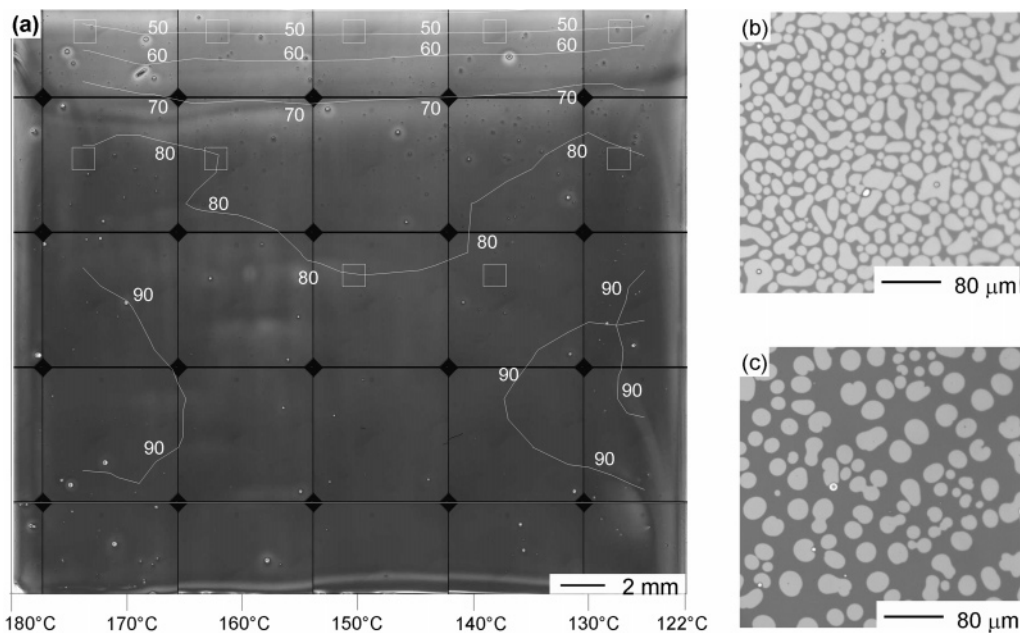


Figure 2. Images of film morphology. (a) Montage of $25\times$ optical micrographs showing the as-cast morphology of a 26K PS-*b*-PMMA thin gradient film where the measured l values have been overlain as contour plots. The temperature gradient used for annealing is given across the bottom. The squares indicate the approximate locations of higher magnification images used for analysis. (b and c) Representative micrographs showing the morphologies observed at higher magnification after an 84.5 h annealing time. Micrographs are acquired for the regions (b) $l = 53$ nm, $T = 175$ °C and (c) $l = 80$ nm and $T = 163$ °C.

patterns by inhibiting long-range order in the system. This effect is analogous to the suppression of long wavelength phase separation in bulk block copolymer materials caused by the covalent junction between the blocks.²⁵

One interesting feature of this phase separation model of pattern formation in block copolymer films is that it predicts potentially dramatic changes in the film pattern morphology through changes in the surface elasticity. In our previous work^{1,2} it was found that the “steady-state” size of the surface features, λ , was strongly reduced as M was increased ($\lambda \sim M^{-1.65}$). Additionally, the surface (bending) elasticity of a BC layer is theoretically predicted^{45,46} to rise sharply ($\kappa \sim M^3$) with increasing M in block copolymer and surfactant films. The observed behavior of λ and the predicted behavior of κ as a function of M imply an inverse scaling between λ and κ . In particular, a relation of $\lambda \sim \kappa^{-0.5}$ was proposed on the basis of previous observations^{1,2} and the theoretical scaling relation between κ and M . This relation reinforces the idea that changes in the surface elasticity can induce changes in the pattern morphology. Finally, the inclusion of κ in the phase separation model implies that T should also effect the BC pattern formation. As T is raised, the film becomes more disordered and κ should drop. The rate at which the system approaches the asymptotic organized pattern state (it is frankly unclear whether this state is an equilibrium state or just a long-lived metastable condition) may also be influenced by order parameter fluctuations near the disordering temperature. The current investigation therefore places particular emphasis on the influence of T variations on the surface pattern size and pattern formation kinetics.

Experimental Section

A symmetric diblock copolymer of polystyrene-*b*-poly(methyl methacrylate) (PS-*b*-PMMA) was purchased from Polymer Source Inc.⁴⁷ and was used as received. The molecular masses (M_n)⁴⁸ of the PS and PMMA blocks were 12.8 and 12.9 kg/mol, respectively, and

$M_w/M_n = 1.05$. The lamellar domain size (L_o) of this polymer is measured to be 18 nm.² Unreacted homopolymer contamination is estimated to be less than 4% based on GPC and NMR data provided by the supplier. A gradient flow coater^{1,2,23,24} was utilized to produce a thin polymer film with a gradient in thickness on Si wafers (Polishing Corp. of America) with an oxide surface produced by “piranha etching”⁴⁹ the wafer. A solution with mass fraction 2% PS-*b*-PMMA in an equal toluene/chloroform mixture was used with a stage acceleration of 5 mm/s² to produce a gradient ranging from 40 to 95 nm in thickness over a lateral scale of 30 mm (1.83 nm/mm average slope). The gradient film thickness was characterized with UV-visible interferometry (0.5 mm diameter with standard uncertainty of ± 1 nm at 500 nm film thickness) on a grid with 2.5 mm spacing. The sample was subsequently placed on a gradient hot stage²³ with the thickness gradient orthogonal to the temperature gradient and annealed under vacuum for 84.5 h over a temperature range of 122–180 °C. The annealing stage was placed on an automated optical microscope, and optical micrographs were digitally captured throughout the annealing process. Low magnification ($\approx 25\times$) images were obtained to provide an overview of the sample, while higher magnification ($\approx 200\times$) images were acquired to monitor the morphological evolution of the sample at higher resolution.

Results

A composite optical micrograph is shown in Figure 2a demonstrating the as-cast morphology of the thin film gradient with l shown in the contour plot displayed over the micrographs. This figure shows a smooth film with a low number of defects and generally increasing l from top to bottom, although the contour lines show that the l -gradient is not linear or uniform. The

(47) Certain equipment and instruments or materials are identified in the paper to adequately specify the experimental details. Such identification does not imply recommendation by the National Institute of Standards and Technology, nor does it imply the materials are necessarily the best available for the purpose.

(48) According to ISO 31-38, the term “molecular weight” has been replaced by “relative molecular mass”, M_r . The conventional notation, rather than the ISO notation, has been employed for this publication.

(49) Kern, W., Ed. *Handbook of Semiconductor Wafer Cleaning Technology*; Noyes Publications: Park Ridge, NJ, 1993.

(45) Wang, Z. G.; Safran, S. A. *J. Chem. Phys.* **1991**, *94*, 679.

(46) Wurger, A. *Phys. Rev. Lett.* **2000**, *85*, 337.

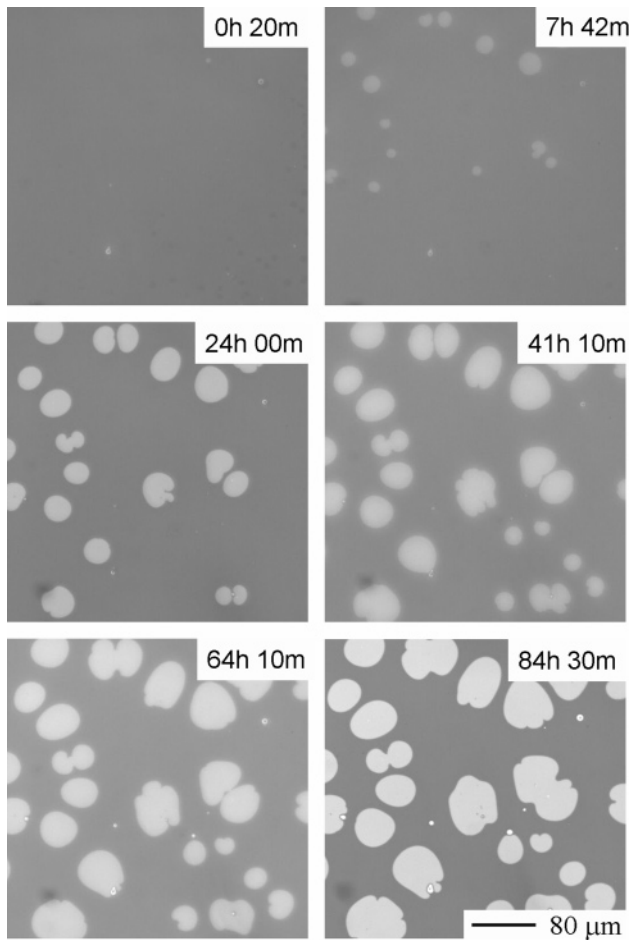


Figure 3. Optical micrographs of the $l = 80$ nm and $T = 175$ °C film area showing the increase in hole size with increasing annealing time. The lighter color corresponds to thinner areas and the scale bar applies to all images.

temperature gradient used to anneal the sample is indicated at the bottom of Figure 2a. The small squares in Figure 2a represent the approximate locations of the higher magnification images acquired during annealing. These micrographs were obtained at temperatures of 127 ± 1 , 139 ± 1 , 151 ± 1 , 163 ± 1 , and 175 ± 1 °C and film thicknesses of 53 ± 3 and 80 ± 3 nm for a total of 10 (l , T) combinations. (The \pm values indicate estimated standard relative uncertainties and this applies to all uncertainty intervals indicated in this paper.) These film thicknesses correspond² to $l = 2.94L_0$ and $4.44L_0$, and the morphologies observed at these thicknesses are shown in Figure 2b,c. These optical micrographs were obtained at 53 nm and 175 °C (Figure 2b) and 80 nm and 163 °C (Figure 2c) after 84.5 h of annealing (the lighter color corresponds to thinner film thicknesses). The morphology observed in Figure 2b consists of a continuous lamella with a large number of holes extending down to the underlying completed lamellae. These holes cover a majority of the sample top surface. (Note that the holes do not correspond to a dewetting morphology, which would correspond to holes passing entirely through the block copolymer film.) For the 80 nm sample (Figure 2c), a similar hole morphology is observed, but with a lower hole density and surface coverage.

A sequence of optical micrographs similar to those in Figure 2b,c was obtained throughout the annealing process to study the kinetics of the surface pattern formation. Figure 3 shows this sequence of micrographs for the $l = 80$ nm film annealed at $T = 175$ °C for times (t) up to 84.5 h. The initial image ($t = 20$

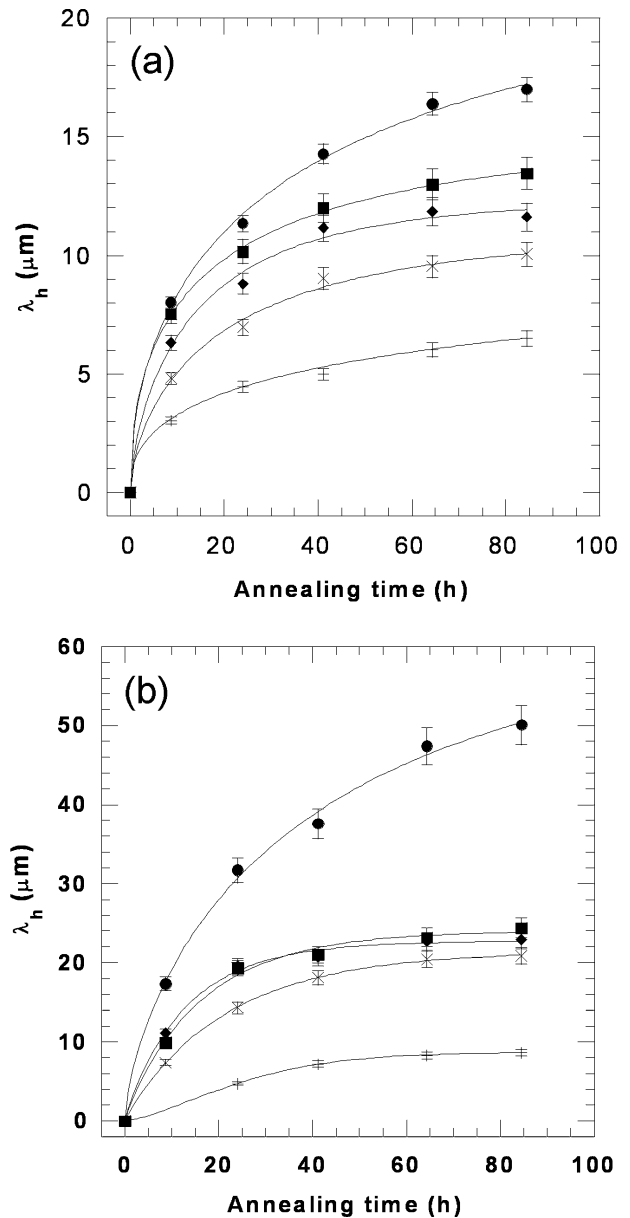


Figure 4. Plots of λ_h for the (a) 53 nm and (b) 80 nm thick films as a function of annealing time and temperature (\bullet , 175 °C; \blacksquare , 163 °C; \square , 151 °C; \times , 139 °C; $+$, 127 °C) with the standard uncertainties displayed. The line represents fits to eq 1.

min) shows a smooth film corresponding to a time when the hole features are not detectable by the optical microscope. After 7 h and 42 min, several holes have formed in the lamella surface and with increasing time they enlarge, with impingement and coalescence observed in some cases. A similar set of micrographs is obtained for each T and l combination shown in Figure 2a. To quantify the growth behavior of the holes, the micrographs are analyzed to determine an average hole diameter, λ_h , as a function of l , T , and t . (Since the holes are not perfectly round in all cases, we determine λ_h by measuring the area of the holes and specifying an effective diameter of a circle with the same area.) The results of this analysis are shown in Figure 4 for both the 53 nm (Figure 4a) and 80 nm (Figure 4b) thickness series. Inspection of these plots reveals that λ_h increases with increasing T and that the 80 nm thick film has larger values of λ_h than the 53 nm films. The variation in the measured values of λ_h due to film thickness is influenced by the relative deviation of l from the characteristic values l_s where smooth films are expected.^{10,12,29} For a 53 nm

Table 1. λ_h Data for Both 53 and 80 nm Thickness Films Obtained from a Fit to Eq 1^a

T (°C)	53 nm			80 nm		
	$\lambda_{h,\infty}$ (μm)	τ (h)	α	$\lambda_{h,\infty}$ (μm)	τ (h)	α
127	10.8 \pm 3.9	101.2 \pm 28	0.44 \pm 0.15	8.7 \pm 0.1	28.1 \pm 0.6	1.47 \pm 0.09
139	11.0 \pm 1.1	21.1 \pm 6.6	0.65 \pm 0.12	21.5 \pm 0.2	21.6 \pm 0.5	0.91 \pm 0.03
151	12.3 \pm 0.9	14.9 \pm 3.4	0.70 \pm 0.15	22.7 \pm 0.6	13.0 \pm 1.2	0.95 \pm 0.13
163	15.3 \pm 0.9	19.1 \pm 4.1	0.51 \pm 0.05	24.1 \pm 0.9	16.2 \pm 1.9	0.94 \pm 0.14
175	22.9 \pm 5.2	45.2 \pm 15	0.53 \pm 0.10	63.6 \pm 12	43.9 \pm 12	0.69 \pm 0.11

^a Uncertainty intervals indicate estimated standard relative uncertainty.

thickness ($l = 2.94L_0$) film, the thickness is just above the value found for the bicontinuous morphology and is approximately shown by arrow A in Figure 1.² In this case, large numbers of holes nearly cover the surface, and pattern growth can only occur at the expense of other holes. In the case of the 80 nm ($l = 4.44L_0$) film, however, l is nearly equal to a value characteristic of smooth films ($l_s = 4.5L_0$), as shown by arrow B in Figure 1.² The holes observed for this film thickness are well-dispersed and can grow in a nearly independent fashion. Next, a model is introduced to quantify the hole growth kinetics.

Previous experimental studies^{13,18,21} have suggested that the holes grow as a power law in time, although the apparent exponents reported were sometimes very small (e.g., 0.08).¹⁸ These empirical forms are consistent with the phase separation model discussed above, where the diffusive nature of transport processes leads to growth and nonlinear interaction effects associated with the competition between the growing species lead to an apparent power law coarsening. This general phenomenon arises in a wide range of pattern formation processes and reasonably extends to a phenomenological description of the early stage of the hole coarsening process in the block copolymer films. This simple picture must break down at long times, however, as the surface structures (holes) approach a steady-state size at long times, an effect we ascribe below to the surface elasticity of the film. Accordingly, the kinetics of the hole growth can be modeled on the basis of two plausible assumptions: (1) a first-order rate law applies at short times, where diffusive coarsening dominates, and (2) a limiting value of the hole size exists at long times, $\lambda_h(t \rightarrow \infty) = \lambda_{h,\infty}(T)$. This combination of physically plausible assumptions yields the following expression for the hole size as a function of time,

$$\lambda_h = \lambda_{h,\infty} \{1 - \exp[-(t/\tau)^\alpha]\} \quad (1)$$

where τ describes the “coarsening time” and α is an exponent governing the rate of coarsening. A fit of this expression to our data is shown as the lines in Figure 4, and the derived parameters ($\lambda_{h,\infty}$, τ , α) are given in Table 1. We see in Figure 5 that the data for $\lambda_h/\lambda_{h,\infty}$ can be collapsed onto a common master curve as a function of $(t/\tau)^\alpha$. This data superposition suggests that similar physical processes govern the hole coarsening for each of the film thicknesses and temperatures studied. In previous studies, a similar argument and data superposition was found to describe the characteristic length scale of phase separation in a surfactant-micelle-forming fluid undergoing phase separation and subsequent ordering^{50–52} and in the description of the coverage kinetics in the diffusion-controlled growth of adsorbed polymer layers on surfaces from solution.^{53,54} In this surface adsorption process,

however, the saturation of the growth process at long times is due to excluded volume interactions rather than elastic effects within these layers.^{53–55}

Inspection of the model parameters summarized in Table 1 reveals some interesting trends. First, the long-time steady-state hole size $\lambda_{h,\infty}$ increases with rising T for both the 53 and 80 nm thickness films, as shown in Figure 6. This result demonstrates that T not only affects the kinetics of pattern formation but the final size of the patterns as well. In addition, the τ values (plotted as a function of T in Figure 7) exhibit an apparent *minimum* around 151 °C. Thus, the initial increase in the growth rate of the holes is followed by a decrease in growth rate as T continues to rise. Our interpretation of these parameter variations with respect to h and T in terms of our working theoretical framework is described in the next section.

Discussion

We first consider the increase in $\lambda_{h,\infty}$ with rising T . As discussed above, an increase in the size of BC surface patterns was also observed as a function of molecular mass ($\lambda_{h,\infty} \sim M^{-1.65}$; fixed T) in our companion work.^{1,2} Although these observations focused on the labyrinthine “spinodal” surface patterns that occur in a narrow film height region between the hole and island formation regions, similar variations in the scale of the islands and holes as a function of M were also found. This behavior is demonstrated in Figure 8, where AFM micrographs obtained at constant magnification of PS-*b*-PMMA copolymers with total M_n of (a) 26 kg/mol, (b) 51 kg/mol, and (c) 104 kg/mol are shown (the lighter color corresponds to a higher topography).⁵⁶ The samples were annealed for 30 h at 170 °C and the film thickness is (a) 59 nm ($3.27L_0$), (b) 68 nm ($2.26L_0$), and (c) 97 nm ($2.30L_0$), respectively. The micrographs show a clear decrease in λ_h with increasing molecular mass, and λ_h is calculated as (a) 4.5 μm , (b) 2.3 μm , and (c) 1.2 μm for these micrographs. This dependence of the hole size on M was previously suggested to be due to the same mechanism as the bicontinuous patterns,^{1,2} namely an increase in the surface elastic constant κ (Helfrich elastic constant)^{43,57,58} of the outer block copolymer layer.

In a similar vein, the observed increase in $\lambda_{h,\infty}$ with rising temperature in the present work is attributed to a decrease in κ with increasing T . Previous observations of κ for small molecule amphiphilic films have shown that κ depends sensitively on the degree of system ordering.^{7,43} Specifically, as the disordering

(53) Douglas, J. F.; Johnson, H. E.; Granick, S. *Science* **1993**, 262, 2010.

(54) Johnson, H. E.; Douglas, J. F.; Granick, S. *Phys. Rev. Lett.* **1993**, 70, 3267. See also: Hubbard, J. B.; Silin, V.; Plant, A. L. *Biophys. Chem.* **1998**, 175, 163.

(55) Douglas, J. F.; Schneider, H. M.; Frantz, P.; Lipman, R.; Granick, S. *J. Phys. Condens. Matter* **1997**, 9, 7699. See also ref. 8.

(56) Further information about the polymer molecular masses of can be found in ref. 2.

(57) Helfrich, W. Z. *Naturforsch C* **1975**, 30, 841.

(58) Jiang, Y.; Lookman, T.; Saxena, A. *Phys. Rev. E* **2000**, 61, R57.

(50) Wilcoxon, J. P.; Martin, J. E.; Odinek, J. *Phys. Rev. Lett.* **1995**, 75, 1558.
(51) Emerton, A. N.; Coveney, P. V.; Boghosian, B. M. *Phys. Rev. E* **1997**, 55, 708.

(52) Nekovee, M.; Coveney, P. V.; Chen, H.; Boghosian, B. M. *Phys. Rev. E* **2000**, 62, 8282.

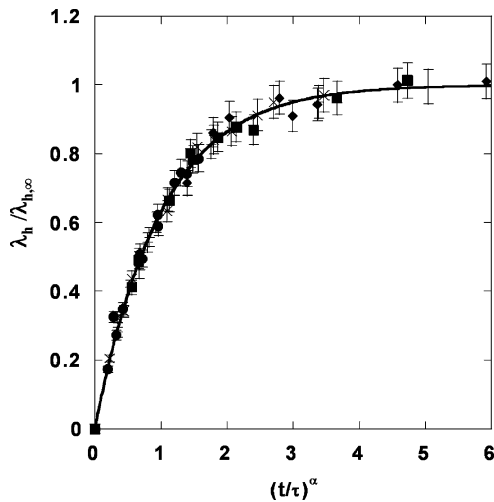


Figure 5. Plot of all the film thickness and temperature (●, 175 °C; ■, 163 °C; □, 151 °C; ×, 139 °C; +, 127 °C) data presented in Figure 4 collapsed to a universal curve. The line represents eq 1.

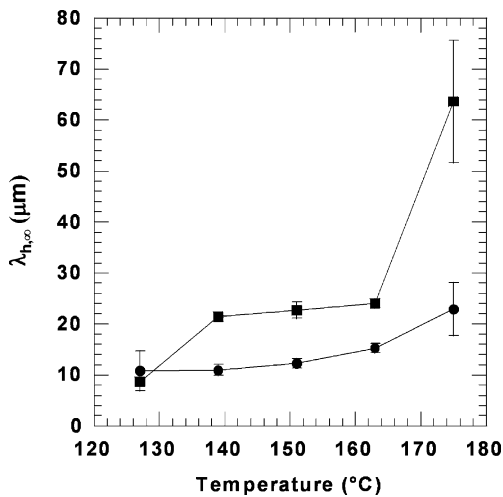


Figure 6. Plot of the steady-state hole size ($\lambda_{h,\infty}$) for the 53 nm (●) and 80 nm (■) thickness films as a function of T . Lines serve as guides for the eye and the uncertainty intervals represent estimates of standard relative uncertainty.

temperature of these films is approached, κ decreases due to thermal fluctuations.^{59,60} We can expect a similar effect in our block copolymer films as T approaches the corresponding disordering temperature T_d , so that lamellar interfaces become more diffuse and thermal fluctuations become large (As we discuss below, the T_d of our block copolymer films is highly sensitive to film thickness, and the precise value of T_d can only be roughly estimated.). At any rate, a reduction in κ with increasing T is quite understandable for ordered films ($T < T_d$), and this trend is consistent with our former interpretation of the M dependence of the surface pattern scale, $\lambda_{h,\infty}$.^{1,2} Specifically, the scaling relation between $\lambda_{h,\infty}$ and κ inferred from our former work (approximately $\lambda_{h,\infty} \sim \kappa^{-1/2}$) indicates a precise relation between the increased surface feature size $\lambda_{h,\infty}$ and T through the T dependence of κ . The monotonic dependence of $\lambda_{h,\infty}$ on T observed in Figures 4 and 6 is exactly the trend expected from this relation. Thus, as T is further increased, the holes are expected to become larger and larger and more irregular in shape, ultimately disappearing when the film fully disorders and has a vanishing surface elasticity.

(59) Helfrich, W. *J. Phys. Fr.* **1985**, *46*, 1263.

(60) Peliti, L.; Leibler, S. *Phys. Rev. Lett.* **1985**, *54*, 1690.

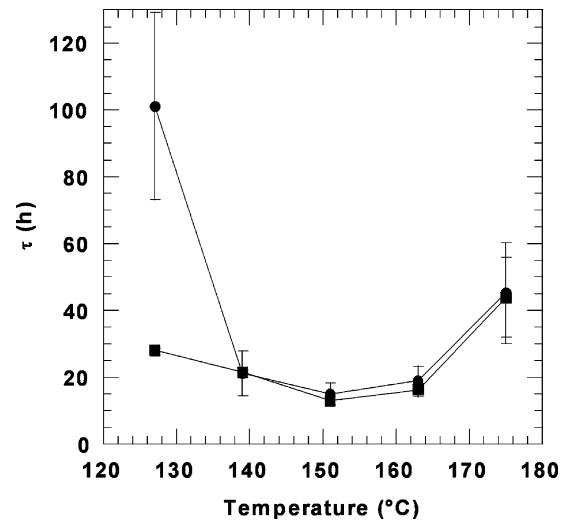


Figure 7. Plot of the time constant τ for the 53 nm (●) and 80 nm (■) films as a function of temperature. The minima correspond to a peak in film mobility. Lines serve as guides for the eye, and the error bars correspond to the fit uncertainty.

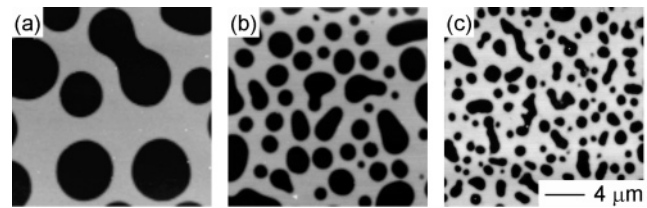


Figure 8. AFM micrographs of surface holes in (a) 26K, (b) 51K, and (c) 104K PS-*b*-PMMA samples annealed for 30 h at 170 °C showing the decrease in λ_h with increasing molecular mass. Lighter regions correspond to higher topography.

Although we only quantify this trend for the surface hole patterns in the current experiment, we expect the same trend to apply to the island and labyrinthine surface morphologies as well. We now focus the discussion on the effect of temperature on the observed time constants describing the surface pattern formation process.

In eq 1, the parameter τ is used as a measure of how fast the pattern formation occurs [when $t = \tau$, the hole size $\lambda_h(t)$ has reached $\{1 - 1/e\}$ of its asymptotic value, $\lambda_{h,\infty}$ or $\lambda_h(t=\tau) \approx 0.63\lambda_{h,\infty}$], so that a large value of τ means the system reaches its asymptotic pattern size slowly. Alternatively, the reciprocal of τ defines the rate of surface pattern formation.

Although caution must be exercised due to the limited number of data points, we propose that the maximum in surface pattern formation rate ($1/\tau$) as function of temperature is due to two basic competing effects that must influence the rate of ordering in block copolymer systems: a reduction in molecular mobility at low temperatures associated with glass formation and a slowing of the rate of ordering due to fluctuation effects associated with an approach to the block copolymer film disordering temperature T_d from below. Thus, increasing temperature at very low temperatures relative to the order-disorder transition causes the mobility to increase,⁶¹ but the mobility then decreases as compositional fluctuations slow down the ordering process as the film-ordering temperature T_d is approached from below. (This interpretation of the slowing down of the dynamics is consistent with the mechanism that we discussed above for the T dependence of $\lambda_{h,\infty}$.) We thus expect to see a nonmonotonic variation in the

(61) Doi, M.; Edwards, S. F. *The Theory of Polymer Dynamics*; Oxford University Press: Oxford, 1986.

rate of BC ordering, and indeed, this type of growth kinetics has been repeatedly observed in the grain growth of polystyrene–polyisoprene block copolymers in relatively thick (bulklike) films diluted by solvents to enhance molecular mobility.⁶² A non-monotonic variation in ordering rate with temperature is a rather general phenomenon that is also observed in the crystallization of polymers and small molecule liquids⁶³ and in the ordering of lamellae in lipid lamellar vesicles.^{64,65}

Although the *qualitative* origin of the peak in the surface pattern ordering rate ($1/\tau$) as a function of temperature is clear, the insensitivity of this peak temperature to film thickness was unanticipated. Moreover, the morphology differences that accompany these l values suggest that the mobility peak is also insensitive to the type of surface pattern formed. This observation raises the question of whether the dynamics of this surface pattern formation might reflect the ordering dynamics of the block copolymer film as a whole. Further work is obviously needed to confirm this possibility, which would establish the significance of τ and the peak surface ordering rate temperature as potentially basic processing parameters relevant to optimizing the fabrication of BC materials by self-assembly. The insensitivity of the peak-ordering rate with film thickness also raises questions about how the thermodynamics of the BC ordering transition becomes modified in such thin films, and we briefly describe some issues that need to be considered in future measurements.

As discussed above, the solid substrate induces order in the BC films, leading to a shift of the film-ordering temperature, T_d .^{16,32,38} Specifically, a power law upward shift of the order–disorder transition temperature with decreasing film thickness,⁶⁶ $[T_d(l) - T_{d,\text{bulk}}] \sim l^\delta$ with $\delta \approx -3$, has been previously reported for our block copolymer system, where a 50–60 °C upward shift of the film-ordering temperature was estimated for the thinnest film considered in these previous studies ($l \approx 90$ nm). A similar large shift in the magnitude of T_d relative to the bulk is in our own films, although the effect is expected to be smaller given the lower molecular mass of our block copolymers. We are then led to the question of why this effect does not lead to a substantial shift in the peak-ordering rate temperature of our surface pattern formation as we vary film thickness.

Interpreting this observation is complicated by the fact that the films are also thin enough to exhibit shifts in the glass transition temperature, as well as in the equilibrium BC ordering temperature, T_d . Despite these complications, these limited observations lead us to question how T_d depends on l in films composed of only a few lamellar layers. Can we extrapolate the shifts found in thicker films⁶⁶ to such thin films? Indeed, theoretical estimates of the shift of the ordering temperature in layered liquid crystal films, which have many features in common with block copolymer films, indicate that the ordering temperature can vary *nonmonotonically* with film thickness if there is a strong ordering effect induced by the boundary interaction.⁶⁷ Moreover, recent self-consistent field calculations for block copolymer ordering in the presence of a neutral interacting boundary show a strong *downward* shift of the ordering temperature under high confine-

ment conditions,⁶⁸ which can be understood to arise as a simple consequence of the reduction of the effective spatial dimensionality (the interchain contacts depend on dimensionality) with strong confinement. On the basis of these observations, and the evident tendency of the boundary interactions to induce ordering in our films, it is highly plausible that T_d might exhibit an *insensitivity* to film thickness over a restricted film thickness range. Evidently, further investigations of the pattern-ordering rate $1/\tau$ over a larger temperature range, glass formation in thin block copolymer films, and a serious effort to determine T_d as a function of l , especially in the regime of small l , is needed to provide a firm basis for interpreting the temperature dependence of the block copolymer ordering rate in thin films.

Finally, we address another variable that is difficult to interpret theoretically, the coarsening exponent α (Table 1). Inspection of these values suggests that α is more sensitive to h than T and tends to take a smaller value in the thinner film ($l = 53$ nm). It is hard to provide a definitive explanation of this trend, but the phase separation model of block copolymer coarsening does provide some direction. First, the fits in Figure 4 emphasize late-stage coarsening kinetics, and different apparent exponents would likely be obtained if short time data were emphasized. We must also appreciate that these films are thin enough that dimensionality effects are relevant. Previous work indicates a crossover between three- and two-dimensional coarsening kinetics of polymer blend phase separation for a film thickness in the range between 20 and 100 nm.⁶⁹ In three dimensions, the late-stage exponent for fluid phase separation is 1 while the exponent is in the range from $1/2$ to $2/3$ for two dimensions.^{51,70–73} The α variations observed seem consistent with this type of crossover from three- to two-dimensional phase separation kinetics. (Of course, other interpretations are possible, but the phase separation model of block copolymer pattern formation remains a viable interpretation of the kinetic data.) This interpretation is potentially upset, however, by the large apparent exponent $\alpha = 1.47$ found for the thicker film ($l = 80$ nm) at $T = 127$ °C. Such an exponent is characteristic of Kolmogorov–Avrami ordering kinetics. Notably a best-fit exponent $\approx 3/2$ has been reported in the ordering kinetics (fraction of material converted to ordered phase rather than pattern size) of multilamellar lipid bilayers.^{74,75} Obviously, further study is required to better resolve the nature of α .

(62) Chastek, T. Q.; Lodge, T. P. *Macromolecules* **2003**, *36*, 7672. Chastek, T. Q.; Lodge, T. P. **2004**, *37*, 4891. Chastek, T. Q.; Lodge, T. P. *J. Polym. Sci. B* **2005**, *43*, 405.

(63) Brandrup, J.; Immergut, E. H.; Grulke, E. A. *Polymer Handbook*, 4th ed.; Wiley-Interscience: New York, 1999. Broughton, J. Q., Gilmer, G. H., Jackson, K. A. *Phys. Rev. Lett.* **1982**, *49*, 1496. See also Figure 4 of Beers, K. L.; Douglas, J. F.; Amis, E. J.; Karim, A. *Langmuir* **2003**, *19*, 3935 and references on this topic cited in this work.

(64) Gershfeld, N. L.; Mudd, C. P.; Tajima, K.; Berger, R. L. *Biophys. J.* **1993**, *65*, 1174.

(65) Gershfeld, N. L. *J. Phys. Chem.* **1989**, *93*, 5256.

(66) Russell, T. P.; Hjelm, R. P., Jr.; Seeger, P. A. *Macromolecules* **1990**, *23*, 890.

(67) Li, H.; Paczusi, M.; Kardar, M.; Huang, K. *Phys. Rev. B* **1991**, *44*, 8274. The exact calculations of the ordering temperature of systems with interacting boundaries in this work suggest that other basic phenomena must be considered in thin block copolymer films than just a nonmonotonic dependence of the order–disorder temperature with film thickness. Specifically, these illustrative calculations show that the ordering process can involve *two* distinct ordering temperatures when the boundary interaction strongly induces ordering in the film, a physical situation that is thought to be prevalent in block copolymer films. These calculations also indicate that the shift of the order–disorder transition temperature can be *strongly dependent on the magnitude of the substrate interaction*, a phenomenon that could have tremendous consequence for the ordering of block copolymer films on chemically patterned substrates. Finally, we point out that a monotonic variation of the critical temperature of blend films (Kumar, S. K.; Douglas, J. F.; Szeifer, I. unpublished) and even the superconductivity transition in thin films (Strongin, M.; Kammerer, O. F. *J. Appl. Phys.* **1968**, *39*, 2509) can exhibit a similar nonmonotonic shift with confinement, so the effect appears to be rather general.

(68) Alexander-Katz, A.; Fredrickson, G. H. *Macromolecules* **2007**, *40*, 475.

(69) Sung, L.; Karim, A.; Douglas, J. F.; Han, C. C. *Phys. Rev. Lett.* **1996**, *76*, 4368.

(70) Bray, A. J. *Adv. Phys.* **1994**, *43*, 357.

(71) Furukawa, H. *Adv. Phys.* **1983**, *34*, 703.

(72) SanMiguel, M.; Grant, M.; Gunton, J. D. *Phys. Rev. A* **1985**, *31*, 1001.

(73) Yu, Y.; Alexander, F. J.; Lookman, T.; Chen, S. *Phys. Rev. Lett.* **1995**, *74*, 3852.

(74) Ye, Q.; vanOsdol, W. W.; Biltonen, R. L. *Biophys. J.* **1991**, *60*, 1002.

(75) Yang, C. P.; Nagle, J. F. *Phys. Rev. A* **1988**, *37*, 3993.

Conclusions

The surface pattern formation in block copolymer and other lamellar-forming materials is a complex phenomenon that remains poorly understood from a fundamental perspective. Since many parameters influence this type of pattern formation, we pursued a combinatorial investigation of this pattern formation as a function of film thickness, annealing time, and temperature in order to establish the basic phenomenology of this growth process. Our study has revealed some new and basic aspects of this type of pattern formation. First, we find that the pattern dimensions (holes were the focus in the present study) approach a constant size at long times, $\lambda_{h,\infty}$. Moreover, we find that $\lambda_{h,\infty}$ increases with temperature so that the surface pattern size is continuously *tunable*. On the basis of these observations, and the observation of a power-law growth of the scale of the pattern size at short times (the typical trend for phase ordering processes), we propose a simple reaction kinetic model to describe the pattern growth and apply the model to our hole growth data. This model allows us to reduce our hole-coarsening data to a universal master curve, and we deduce that the relaxation time τ governs the pattern

growth. Unexpectedly, τ exhibits a minimum as a function of temperature, which in hindsight is not surprising, since a similar phenomenon is normally observed in crystallization and many other condensed matter ordering processes due to a competition between viscous and thermodynamic factors on the rate of ordering. Indeed, a nonmonotonic temperature dependence of the ordering rate well below the order–disorder temperature has been observed before in the ordering of bulk block copolymer materials.⁶² The temperature dependence of the asymptotic surface pattern scale is interpreted to arise from a variation of the surface elasticity with temperature, an interpretation consistent with our earlier interpretation of the variation of surface pattern size with molecular mass.^{1,2} We also find support for a phenomenological model of block copolymer pattern formation based on a phase separation model, subject to the constraint of a molecular mass- and temperature-dependent surface bending elasticity (Helfrich elastic constant) of the outer block copolymer layer.

LA701084X